

Electronic Supplementary information (ESI)

Efficient mesoporous silica-titania catalysts from colloidal self-assembly

Alexander Sachse, Vasile Hulea, Krassimir L. Kostov, Nathalie Marcotte, Maria Yu. Boltoeva, Emmanuel Belamie and Bruno Alonso

Table of contents

1. Additional experimental details	1
1.1 Characterization techniques	1
1.2 Preparation silica-titania hybrid materials.....	2
1.3 Typical procedure for oxidation of sulfur compounds.....	3
2. Further characterization of the silica-titania.....	3
2.1 Nitrogen sorption.....	3
2.2 Sorption of phenylphosphonic acid (PPA).....	4
2.3 Granulometric study.....	5
2.4 XRD spectra of materials	6
2.5 Diffuse reflectance UV-vis spectra	7
3. Oxidation of sulfur compounds.....	7

1. Additional experimental details

1.1 Characterization techniques

Dynamic Light Scattering (DLS) measurements of colloids size were realized using a Malvern Autoziser 4800 apparatus.

Elemental analyses were done on nano-composites at the CNRS facility “Service Central d’Analyse” (Vernaison, France).

Nitrogen sorption isotherms were recorded using a Micrometrics Tristar apparatus at 77 K. Calcined samples were outgased at 523 K at $3 \cdot 10^{-3}$ Torr for at least 8 h. The pore volume fractions ϕ_{POR} were estimated using the maximum adsorbed volume of nitrogen sorption isotherms considering a density of 2.2 g cm^{-3} for silica. Specific surface areas (S_{BET}) were calculated using the BET method.¹ Average pore diameters were inferred from the nitrogen desorption branch according to Broekhoff and de Boer (BdB).²

Transmission Electron Microscopy (TEM) analyses were made on a JEOL 1200 EX2 microscope operating at 100 kV. Calcined samples were grounded and embedded in a resin and cut into slices (~70 nm thick) with an ultramicrotome.

Scanning Electron Microscopy (SEM) images were recorded using a Hitachi S-4500 I SEM.

¹ S. Brunauer, P. H. Emmett, E. Teller, Adsorption of gases in multimolecular layers. *J. Am. Chem. Soc.* 1938, **60**, 309.

² J. C. P. Broekhoff, J. H. De Boer, Studies on pore systems in catalysts: XIV. Calculation of the cumulative distribution functions for slit-shaped pores from the desorption branch of a nitrogen sorption isotherm. *J. Catal.* 1968, **10**, 377.

Diffuse reflectance UV-vis (DR UV-vis) spectra were recorded under ambient conditions on a Perkin Elmer Lambda 14 spectrometer equipped with a BaSO₄ coated integration sphere. Samples were diluted in BaSO₄; spectra were plotted using Kubelka-Munk function.

³¹P MAS NMR spectra were recorded on a Varian 400 spectrometer operating at a Larmor frequency of 162 MHz. Samples inside 3.2 mm rotors were spun at the magic angle, at frequencies ranging between 18 and 20 kHz. Acquisition conditions were: single 45° pulses, proton decoupling and 5 s recycling delays. Between 1000 and 3000 scans were recorded for each sample. Chemical shifts were referenced towards external H₃PO₄. Tentative assignment comes from previous works.³

X-ray photoelectron spectroscopy (XPS) measurements were carried out on an ESCALAB Mk II (VG Scientific Ltd) electron spectrometer with base vacuum in the analysis chamber of 10⁻⁸ Pa. The XPS spectra were recorded using a Mg K α excitation source with photon energy of 1253.6 eV. The photoemitted electrons were separated, according to their kinetic energy, by a 150° spherical analyzer with a pass energy of 20 eV and 6 mm entrance- and exit-slit widths, which gives a total instrumental resolution of 1.06 eV (as measured with the FWHM of Ag3d5/2 photoelectron line). Due to the small Ti concentrations the Ti2p region was also measured with pass energy of 50 eV in order to increase the signal. Energy calibration was performed by normalizing the C 1s line of adventitious adsorbed hydrocarbons to 285 eV. The relative concentrations of the different chemical species were determined by normalization of the areas of the corresponding photoelectron peaks by their photoionization cross-sections calculated by Scofield.⁴ Grain size was measured by light scattering on a MALVERN Mastersizer 2000 in water dispersions.

1.2 Preparation silica-titania hybrid materials

Chitin flakes extracted from shrimp shells were kindly provided by France Chitin.⁵ Aqueous suspensions of α -chitin nanorods were prepared following a procedure described elsewhere, based on the hydrolysis of chitin in boiling HCl (4 M) for 120 min. The nanorod preparation involves elimination of excess HCl by dialysis, followed by ultrasound dispersion prior to the purification by low- and high-speed centrifugation cycles and suspension in HCl (10⁻⁴ M)/EtOH (1:1) to obtain a 3.3 wt% solution.

An alcoholic solution containing siloxane oligomers (3 mmol.g⁻¹) was obtained by mixing under reflux (4 h) TEOS (ABCR, purity > 99.9%) and water in absolute ethanol (Sigma-Aldrich, purity > 99.8%) with the molar composition 1 TEOS: 2 H₂O: 2 EtOH. The resulting siloxane oligomers are small colloids with an average hydrodynamic diameter of $D_h = 2.9 \pm 0.2$ nm determined by DLS.

For the preparation of the silica-titania hybrid materials the siloxane solution was mixed with Ti(OiPr)₂(acac)₂ (Sigma-Aldrich, 75wt% in isopropanol) and the chitin suspension. The reactant proportions are set to reach the water-ethanol azeotrope composition (ca. 96wt% ethanol) and a given chitin volume fraction ϕ_{CHI} in the final nano-composites.

³ P. H. Mutin, V. Lafond, A. F. Popa, M. Granier, L. Markey and A. Dereux, *Chem. Mater.* 2004, **16**, 567.

⁴ J. H. Scofield, *J. Electron Spectrosc. Relat. Phenom.*, 1976, **8**, 129.

⁵ <http://www.france-chitine.com>

For a typical procedure, in order to obtain a material with $\phi_{\text{CHI}} = 0.65$ and 5 mol% Ti, the siloxane suspension (3 g, $n_{\text{Si}} = 8.88$ mmol) was placed in a round bottom flask (1 l) and stirred. $\text{Ti}(\text{OiPr})_2(\text{acac})_2$ (0.228 g, $n_{\text{Ti}} = 0.469$ mmol) was added dropwise at RT. The yellow mixture was stirred for additional 5 min and the chitin solution (22.5 ml) was added dropwise forming a yellow/orange paste. The paste was dissolved by adding 400 ml of absolute ethanol. The solvent mixture is evaporated using standard rotary evaporation conditions until the solution transforms into a paste. The same initial amount of ethanol is then added and the mixture is again evaporated. These solvent-exchange cycles are repeated three times to ensure complete removal of water. After the last ethanol removal, the resulting paste was dissolved in ethanol in order to achieve a chitin concentration of $3 \cdot 10^{-3}$ g.ml⁻¹. Microparticles were obtained by spray-drying the obtained suspension using a Büchi 290 mini-spray dryer under dry nitrogen at 393 K. Mesoporous samples were obtained by calcination in air (8 h, 823 K).

1.3 Typical procedure for oxidation of sulfur compounds

For the oxidation reactions, methyl-phenyl sulfide (Sigma-Aldrich, purity > 99%) and dibenzothiophene (Sigma-Aldrich, purity > 98%) were used as purchased without further purification. The catalytic experiments were carried out at atmospheric pressure in a three-neck glass batch reactor (50 mL), equipped with magnetic stirrer and thermometer immersed in an oil bath. In a typical experiment, the solid catalyst (50 mg) was suspended under stirring (1000 rpm) in a mixture containing the organic sulfur component (1.5 mmol), and acetonitrile (Fisher Chemical, HPLC Gradient grade, 15 mL) as solvent. The mixture was heated to 60 °C and hydrogen peroxide (Sigma-Aldrich, 50 wt% aqueous solution, 3 mmol for MPS and 7.5 mmol for DBT) was added at once. Blank experiments were carried out by mixing the reactants in absence of catalyst. Samples were periodically withdrawn from the reaction mixture, filtrated and analyzed on a Varian 3900 chromatograph equipped with a capillary column (DB-1, 60 m, 0.20 mm id, 0.25 μm film thickness).

2. Further characterization of the silica-titania

2.1 Nitrogen sorption

The nitrogen sorption isotherms at 77 K of calcined materials prepared with ϕ_{CHI} of 0.15, 0.25, 0.33, 0.5 and 0.65 with 5 mol% Ti are shown in Fig. S1. It should be noticed that for the material synthesized with $\phi_{\text{CHI}} = 0.65$ larger mesopores are formed (through interconnectivity of the separated pores) that can favour mass transfer.

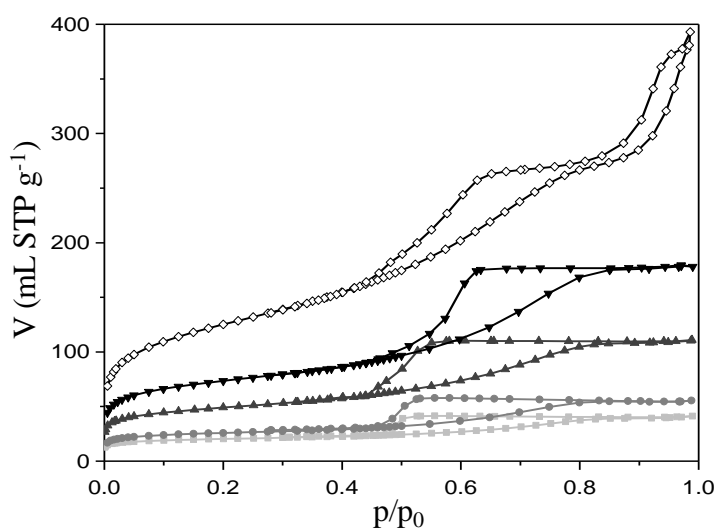


Fig. S1. Nitrogen Sorption isotherms (■, ●, ▲, ▼, ◇ correspond to calcined materials synthesized with ϕ_{CHI} 0.15, 0.25, 0.33, 0.5 and 0.65, respectively).

The textural properties for the synthesized materials inferred from the isotherms in figure S1 are gathered in table S1.

Table S1. Textural properties of calcined materials with 5mol% Ti.

Initial ϕ_{CHI}	ϕ_{POR}	S_{BET} ($\text{m}^2 \text{g}^{-1}$)	V (mL g^{-1})	Average pore size (nm)
0.15	0.10	72	0.06	5
0.25	0.17	91	0.09	5.1
0.33	0.24	170	0.17	5.4
0.50	0.34	256	0.27	5.7
0.65	0.44	443	0.60	6

Textural properties as surface area, pore volume and pore size increase with increasing chitin content as more templating material is added during synthesis and can thus be removed upon calcinations. The slight increase in average pore size can be explained by increasing interconnectivity of the pores with increasing chitin content.

2.2 Sorption of phenylphosphonic acid (PPA)

As described in the main text, the accessibility of the Ti sites was assessed by the sorption of PPA on the synthesized samples. These samples were analyzed by ^{31}P MAS NMR and XPS spectroscopy.

In agreement with the literature,³ ^{31}P NMR spectra recorded for a series of samples with constant $\phi_{\text{POR}} = 0.24$ and varying Si/Ti ratios presented the signals of PPA bound to one or more surface sites.

Samples with low amount of Ti show two peaks: one ascribable to $\text{Ph-P}(\text{OTi})_{3-x}(\text{OSi})_x$, and the other one to $\text{Ph-P}(\text{OTi})_3$ species. For samples with increasing amount of Ti ($\text{Si}/\text{Ti} \leq 9$) the peak for the $\text{Ph-P}(\text{OTi})_{3-x}(\text{OSi})_x$ decreases (Fig. S2).

From XPS, the ratio of accessible Ti sites can be assessed. For the sample with $\phi_{\text{POR}} = 0.10$, a P/Ti ratio of 0.2 was found, whilst the sample with $\phi_{\text{POR}} = 0.24$ gave a P/Ti ratio close to 0.6. It is to note that for samples of $\phi_{\text{POR}} > 0.24$, P/Ti ratio stays constant at 0.6. Hence the accessibility to the Ti sites is limited for materials having $\phi_{\text{POR}} < 0.24$.

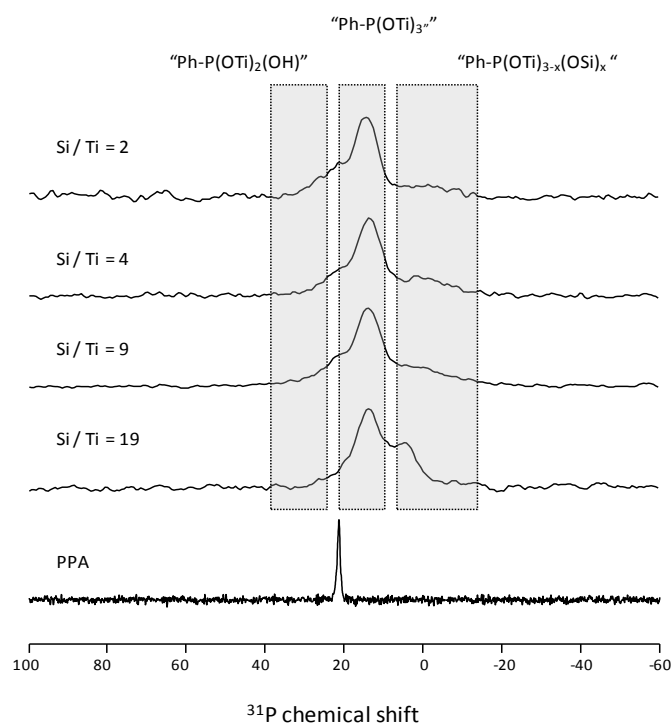


Fig. S2. ^{31}P MAS NMR spectra of materials with constant $\phi_{\text{POR}} = 0.24$ and varying Si/Ti ratios and of the probe molecule PPA.

2.3 Granulometric study

The size distributions of the selected samples have been estimated by granulometry. Fig. S3 evidences the size distributions of obtained particles for three samples ($\phi_{\text{POR}} = 0.4$ and $\text{Si}/\text{Ti} = 19$, $\phi_{\text{POR}} = 0.4$ and no Ti and $\phi_{\text{POR}} = 0.17$ and $\text{Si}/\text{Ti} = 19$). All the size distributions are comparable (similar Log-Normal distribution type) with average particles' diameters between 2.2 and 2.8 μm . The slight differences observed between $\phi_{\text{POR}} = 0.4$ and 0.17 can be due to the changes in the morphology of the particles discussed in the main text.

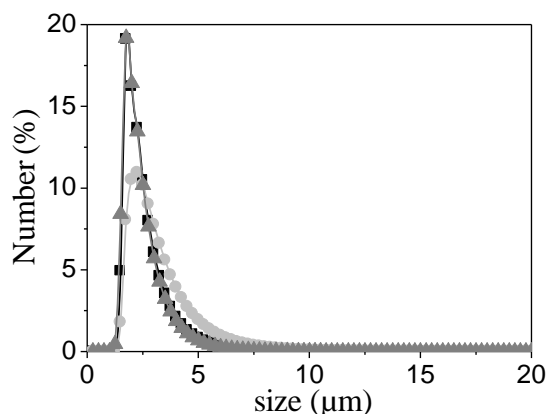


Fig. S3. Experimental size distribution of spray-dried calcined samples (■: $\phi_{\text{POR}} = 0.4$ and Si/Ti = 19, ▲: $\phi_{\text{POR}} = 0.4$ and no Ti, ●: $\phi_{\text{POR}} = 0.17$ and Si/Ti = 19).

Table S2. Experimental and modelled microparticle size distributions of spray-dried calcined samples.

ϕ_{POR}	0.4	0.4	0.17
Si/Ti	∞	19	19
Ti (%)	0	5	5
<i>Experimental data</i>			
D_{average} (μm)	2.21	2.25	2.82
<i>Data modelled using a Log-Normal distribution</i>			
D_{GM}^* (μm)	2.13 ± 0.03	2.18 ± 0.02	2.75 ± 0.02
S_{G}^* (μm)	0.26 ± 0.01	0.26 ± 0.01	0.35 ± 0.01

* Geometric mean diameters D_{GM} and geometric standard deviations S_{G} obtained from the simulation of the size distribution by a log-normal function ($\text{fLN}(D) \sim \exp[2(\ln(D/D_{\text{GM}}))^2/2S_{\text{G}}^2]/(DS_{\text{G}}(2\pi)^{0.5})$).

2.4 XRD spectra of materials

Figure S4 shows the XRD patterns of the sample synthesized with $\phi_{\text{CHI}} = 0.65$ and a Si/Ti ratio of 19. The as-synthesized hybrid material shows wide angle diffracting peaks, that are related to chitin nanocrystals and disappear after calcination. The spectrum recorded with the calcined sample shows the presence of an amorphous phase.

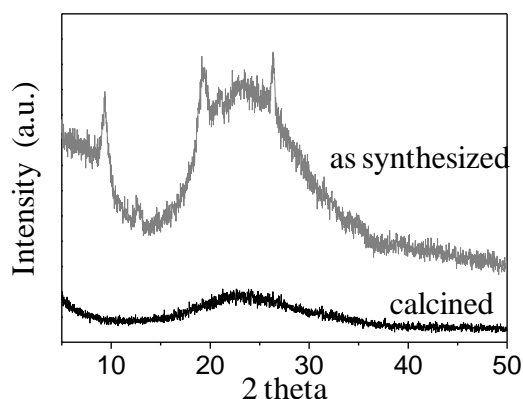


Fig. S4. XRD patterns of as-synthesized and calcined materials ($\phi_{\text{CHI}} = 0.65$, Si/Ti = 19).

2.5 Diffuse reflectance UV-vis spectra

The DR UV-vis spectra of the SiO₂-TiO₂ hybrid materials were compared to the one of pure TiO₂ (anatase). As expected the spectrum of pure TiO₂-anatase shows a characteristic absorption band split into two maxima near 245 and 315 nm with a well defined absorption edge at 390 nm. These features agree with typical TiO₂-anatase spectra⁶ and are related to the O₂--Ti⁴⁺ charge transfer. In contrast, the spectrum for the calcined SiO₂-TiO₂ materials shows a main absorption band at 210 nm and a shoulder at 260 nm.

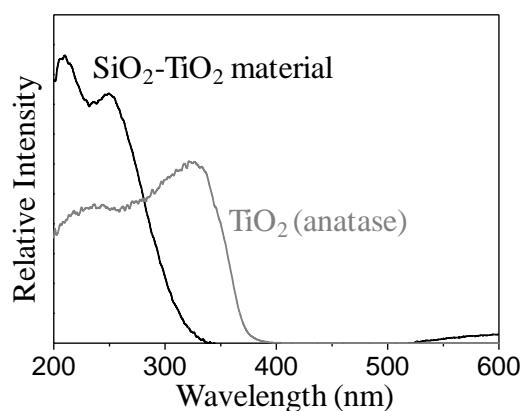


Fig. S5. Diffuse reflectance UV-vis spectra of calcined SiO₂-TiO₂ materials ($\phi_{\text{CHI}} = 0.44$, Si/Ti = 19). (black line) and commercial TiO₂ anatase (grey line).

3. Oxidation of sulfur compounds

The reaction profiles for the oxidation of MPS with hydrogen peroxide over the catalyst with Si/Ti = 19 and $\phi_{\text{POR}} = 0.44$ show conversions with simultaneous apparition of mono- and di-oxidized products. After 10 min of reaction, the amount di-oxidized product increases to the expense of the mono-oxidized product (Fig. S6a). In contrast, the oxidation of DBT shows no apparition of mono-oxidized product throughout the reaction (Fig. S6b).

⁶ J. M. Gallardo-Amores, T. Armaroli, G. Ramis, E. Finocchio, G. Busca, *Appl. Catal. B.*, 1999, **22**, 249.

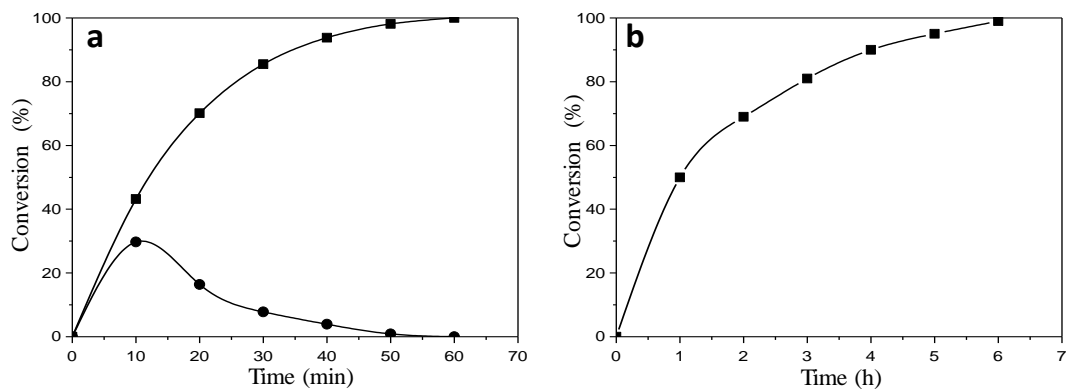


Fig. S6. Conversion of MPS (a) and DBT (b) as function of time. Mono-oxidized (●) and di-oxidized (■) product.

The DR UV-vis spectra of the catalyst with Si/Ti = 19 and $\phi_{\text{POR}} = 0.44$ were recorded before and after the catalytic reaction (Fig. S4).

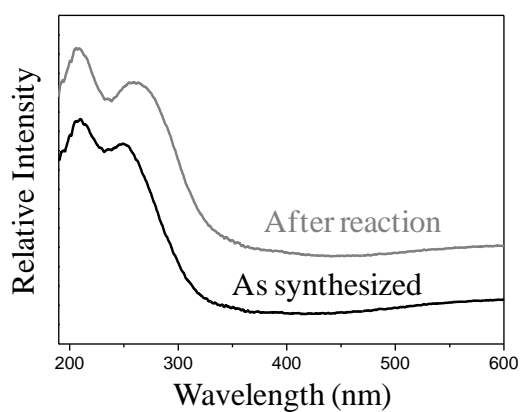


Fig. S7. Diffuse reflectance UV-vis spectra of catalyst before (black line) and after reaction (grey line).